Volume 1 Issue 1 (September 2021)
DOI 10.24191/jaeds.v1i1.35
eISSN 2805-5756

Journal of Applied Engineering Design & Simulation

Simulation of Wire and Arc Additive Manufacturing of 308L Stainless Steel with ColdArc Gas Metal Arc Welding

N. I. S. Hussein[1,*], N. A. N. Jmmani[1], M. N. Ayof[1], T. Abd Rahim[1], M. Z. Zainal Abidin[1], F. Yusof[2], M. F. Jamaludin[2] and S. Williams[3]

[1]Faculty of Manufacturing Engineering, Universiti Teknikal Malaysia Melaka, Hang Tuah Jaya 76100 Durian Tunggal, Melaka, Malaysia.
[2]Faculty of Engineering, Universiti Malaya, 50603, Kuala Lumpur, Malaysia.
[3]Welding Engineering & Laser Processing Centre, Cranfield University, College Road, Cranfield, MK43 0AL, United Kingdom
*corresponding author: izan@utem.edu.my

ABSTRACT

This research focuses on the capabilities of coldArc GMAW in the behaviour of heat input to the weld bead dimension. This study investigated the effect of process GMAW on 308L stainless steel filler wire with a thickness of 1.2 mm and 304L stainless steel base plate, and a dimension of 120 mm x 25 mm x 10 mm (height x width x thickness) by applying WAAM. The data were collected using MATLAB of a Smart Weld Rosenthal's Steady-State 3D Isotherms. A Taguchi response was used in the DOE method with Minitab software to analyse the effect of process parameters on height, width, and depth of weld bead dimension during GMAW. The experiments were conducted following the low, mid, and high input parameters that showed different structures of weld bead dimension, which include 70 A, 75 A, and 78 A (arc current), 15 V, 16 V, and 17 V (voltage), 400 mm/min, 600 mm/min, and 800 mm/min (welding speed). Hence, the optimum value was 75 A, 16 V, and 800 mm/min, while the most significant parameters to deposit stainless steel with coldArc GMAW were welding speed followed by arc current and voltage.

Keywords : wire and arc additive manufacturing, GMAW, 308L stainless steel, MATLAB, taguchi

Nomenclature (Greek symbols towards the end)

I	arc current (A)
V	voltage (V)
v	welding speed (mm/min)

Abbreviations

AM	additive manufacturing
ANOVA	analysis of variance
DOE	design of experiment
GMAW	gas metal arc welding
OA	orthogonal array
WAAM	wire and arc additive manufacturing
S/N	Signal-to-noise ratio

1.0 INTRODUCTION

The WAAM is a layer-by-layer manufacturing process; a form of AM that uses an electric arc to melt the metallic wire. When it comes to AM technology, WAAM can create parts in less time (time-efficient) and at a cheaper cost than other related technologies (cost-competitive) [1-3]. Moreover, according to [4], this technology is a powerful technique with high feed rate. In recent years, research on WAAM technology has primarily focused on WAAM complex component manufacturing, whereby industries commonly make use of arc welding method of GMAW that has been formed, distributed and in trend due to its high weldment strength and decreased post-weld cleaning [5].

GMAW is reported as the second fastest growing welding process. The welding variables that affect the weld penetration, bead geometry, and overall weld quality must be controlled during a manual welding process. Weld bead dimension problems, on the other hand, can be significantly affected by welding procedures and techniques. At the

Received on 17.09.2021
Accepted on 05.10.2021
Published on 13.10.2021

moment of arc re-ignition in coldArc welding, the power output is substantially lower than in a standard short arc technique. Hence, the welding quality issues of height weld, maximum width, and penetration depth are being complied [6]. According to Stuzer et al. [7], standard GMAW enables selecting an optimal process variant based on the required component wall thickness. Pulsed arc welding is an alternative for thick-walled components, whereas for thin-walled structures, the GMAW WAAM technique is advised [8-9]. ColdArc GMAW has several benefits, including minimal heat input, a small heating area, and good thermal stability.

Recent advancement has seen GMAW as an excellent welding method for stainless steel. Due to stainless steel's larger thermal expansion, lower thermal conductivity and lower melting temperature, lower current levels may be preferable to weld mild steel. The carbon and any other alloy composition of welding steel determine the hardness and hardenability of the weld metal, which influences the amount of preheating required. The steel deposits are used to find the best GMAW parameters for better weld efficiency [4], [8] by transforming the experimental results (S/N) ratios since this technique recommends deviating desired values and measured characteristics. Sabdin et al. [10] and Ghosh et al. [11] stated that DOE helps to regulate factors on the relationship by giving a detailed analysis. DOE techniques can minimize the cost of design by speeding up process design, reducing design changes, and reducing material and labour complexity. For DOE, it can understand and control the analysis of variance in order to control and comprehend its ANOVA whereby it acts upon a combination of statistical models to produce an optimal process of parameters in differencing between the mean groups and associate procedures. It provides information on each controlled parameter towards the quality.

The coldArc approach will be beneficial to the industry by reducing costs and lead times, improving material efficiency, improving component performance, and reducing inventory and logistics costs through local usage. On-demand manufacturing claimed that this technology of coldArc AM, which has found its application in the aerospace industry, can cut time to market and material waste and time [12-13]. The capacity to generate massive metal 3D printed pieces and utilize light materials, such as titanium, adds to this attractiveness. For example, for medium-to-large scale engineering components of medium complexity, coldArc with AM provides tremendous cost and lead time-saving potential [6-7]. In addition, WAAM design can offer some topological optimization, while careful wire feedstock selection can enable additional material optimization and multi-material components. The deposited weld metal generates a bead shape on the material. Thereby, the control of weld bead geometry of WAAM is critical.

Hence, this study aims to study the effect of coldArc GMAW parameters that are current, voltage, and travel speed of AM process to the 308L steel single layer bead dimensions on weld bead deposits through Smart Weld simulation in order to optimize the parameters of 308L steel single bead layer deposits for the WAAM process using the Taguchi method whereby the height and width are the primary focuses when determining the size and shape of a weld bead [14]. The voltage parameter in a welding arc is utilized to influence the weld bead form. Besides, the arc current has the most influence on the width of the bead, but the welding speed has the most significant influence on the depth of the bead [15]. The technique has been widely used to overcome the weaknesses of standard GMAW with high heat penetration, making the coldArc approach an excellent alternative.

2.0 METHODOLOGY

2.1 Materials

This research used the 304L stainless steel base plate and 308L stainless steel filler wire for the GMAW WAAM process. The nominal composition of the materials is shown in Table 1 and Table 2. Stainless steel is the commonly used material for reactor coolant pipelines, valve bodies, and pressure vessels. Furthermore, its outstanding high temperature mechanical and corrosion resistance qualities are also employed in the chemical and process industries petrochemical industries. The data were collected and simulated using the SmartWeld software.

Table 1: Nominal composition of grade 308L stainless steel as filler wire and 304L stainless steel for base plate [15]

Elements/Contents (%)	308L Stainless Steel	304L Stainless Steel
Iron, Fe	Balance	Balance
Chromium, Cr	18.95	18.2
Nickel, Ni	10.55	10.0
Manganese, Mn	0.50	2.0
Silicon, Si	0.90	1.0
Phosphorus, P	0.018	0.045
Carbon, C	0.030	0.030
Sulphur, S	0.015	0.030
Copper, Cu	0.1	-
Molybdenum, Mo	0.30	-

2.2 Design of Experiment (DOE)

The welding parameters of welding speed included the low, mid, and high of arc current (A), arc voltage (V), and welding speed (mm/min) as listed in Table 2. The design matrix of the experiments was generated using Minitab® Software v19.0, as shown in Table 3.

Table 2: The selection of response and variable of experimental design

Welding Parameters	Low	Medium	High
Arc Current, I (A)	70	75	78
Voltage, V (V)	15	16	17
Welding Speed, v (mm/min)	400	600	800

Table 3: Taguchi design matrix of L9 orthogonal array

Experiment	Arc Current (A)	Voltage (V)	Welding Speed (mm/min)
1	70	15	400
2	70	16	600
3	70	17	800
4	75	15	600
5	75	16	800
6	75	17	400
7	78	15	800
8	78	16	400
9	78	17	600

The three critical variables of penetration, deposition rate and bead shape were examined in-depth among the welding factors. The findings were evaluated to determine the optimal parameter for a single weld bead deposit. In order to determine the changes in weld bead dimension, three parameters were presented with the lowest, medium, and highest values. The test was then performed, and the results were obtained using a Taguchi of L9 DOE. In this research, the Taguchi design L9 (OA) with 9 runs was applied to optimize the welding parameters of single layer bead deposits to optimize which arc current, voltage, and welding speed offer high weld bead height and wider width and low depth of penetration. The most optimum value was determined from Table 3. The DOE divides the parameters into potential combinations based on the number of components involved and records the experiment's results. By resolving the issues that arise, this technology could save us a significant amount of cost. Typically, humankind has difficulty balancing parameter combinations. However, this tool can generate alternative combinations in seconds after the data were provided. This program can also determine the causes and effects relationship and, in the end, recommend the optimum set of parameters. This tool is required in an experiment to manage the process inputs to achieve optimal results. Current, voltage, and arc welding speed are the parameters involved for this experiment, in which all are modified with three levels each.

2.3 Experimental setup

Firstly, the material of 304L as the base plate was selected from the software, followed by the welding speed and the input power. Power was presented as arc current times by voltage which has to be set up following the parameter used. Then, the plate thickness, view height, and view width were also set up. Finally, after all the parameters were set up, the results data appeared after the 'push to compute contours' button was clicked.

Three-level degrees of welding speed and power input were available for GMAW welding. The simulation was analysed three times based on the three levels of parameters, as shown in Table 4. SmartWeld software was used to create the fusion or moving heat source steady-state conduction model. The effect of process parameters on the output simulated results of height, width, and depth of penetration of weld bead dimension during GMAW welding was later optimized using the Taguchi approach by using Minitab Statistical Software.

Table 4: Process parameter inserted into the simulation software

No.	Smart Weld Parameters	First Level	Second Level	Third Level
1.	Welding Speed (mm/sec)	0.1111	0.1667	0.2222
2.	Input Power (Watts)	1050	1200	1326

3.0 RESULTS AND DISCUSSION

Figure 1 shows the simulated heat distribution for three level parameters to study the effect of coldArc GMAW parameters: current, voltage, and welding speed of the WAAM process to the 308L steel single layer bead dimensions. The weld bead dimension was shown in red colours which indicated the molten metal or fusion zone. The temperature contours bordering the weld zone were in blue colour. Table 5 shows the data collected using the SmartWeld software and the steps of the data collected.

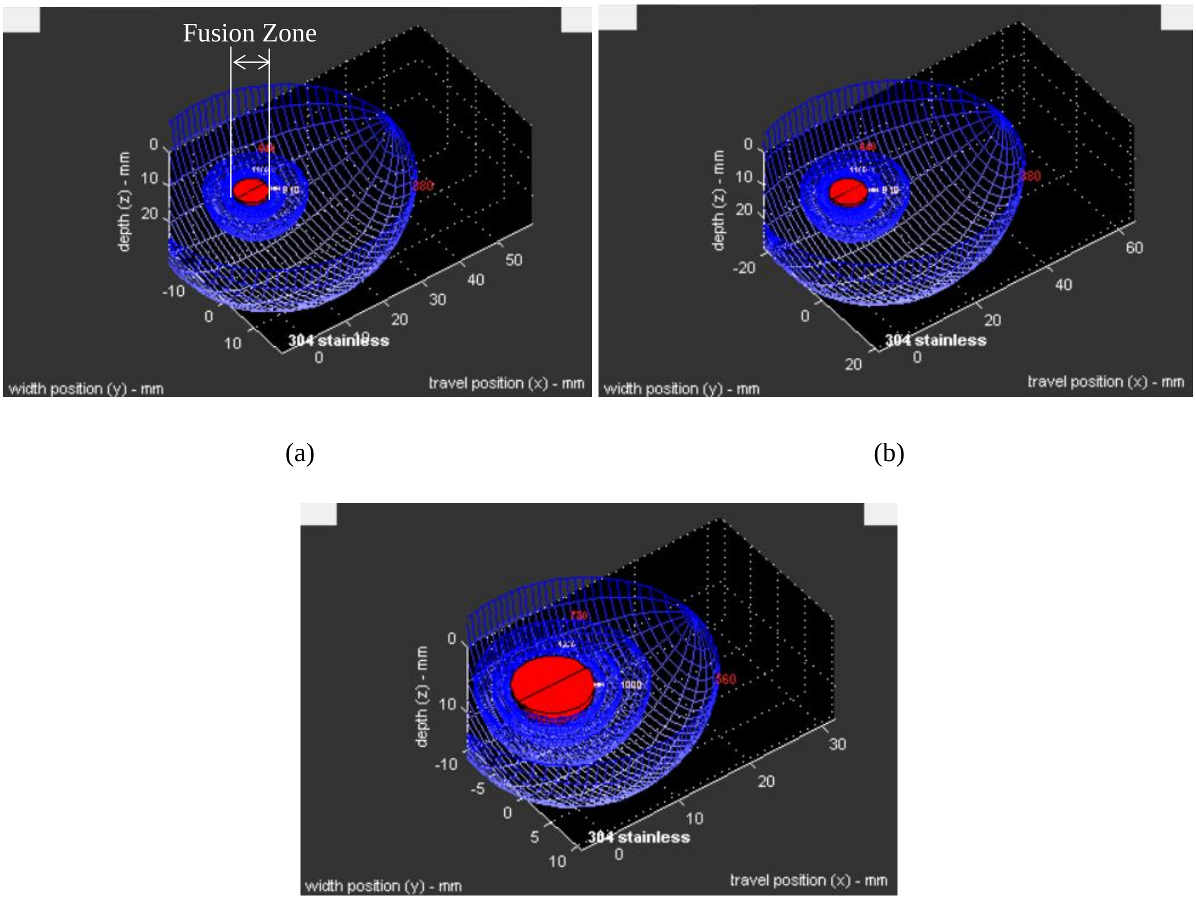

(a) (b)

(c)

Figure 1. Heat Distribution for (a) First Level; (b) Second Level; and (c) Third Level Parameters

Table 5: Simulation result of weld height, weld width, and depth of penetration

Experiment	Arc Current (A)	Voltage (V)	Welding Speed (mm/min)	Weld Height (mm)	Weld Width (mm)	Depth of Penetration (mm)
1	70	15	400	13.5	13.5	3.80
2	70	16	600	22.1	21.8	4.87
3	70	17	800	59.2	56.2	6.73
4	75	15	600	24.7	24.0	5.53
5	75	16	800	64.6	58.3	7.56
6	75	17	400	15.3	15.1	4.35
7	78	15	800	31.9	30.1	7.15
8	78	16	400	14.5	14.3	4.67
9	78	17	600	19.9	19.3	5.63

3.1 ANOVA

The ANOVA was used to assess the differences in variables between mean groups. The contribution of each process parameter to the overall response variation was calculated using the ANOVA approach. In addition, it was used to figure out the importance of each input variables. Minitab® Statistical Software version 19.0 was used in this study to determine the importance of welding factors such as arc current, voltage, and welding speed.

Table 6, Table 7, and Table 8 show that welding speed was the most critical factor in the welding process. Thus, when the F value was considerable, welding speed was the most significant parameter with the largest value from the ANOVA table, which were 12.63, 12.72, and 162.31 for weld height, weld width, and depth penetration, respectively; thus the welding speed substantially impacted the performance characteristic.

Table 6: ANOVA table of weld height

Source	Degree of Freedom	Sum of Squares	Mean	F-Value	P-Value
Arc Current	2	263.9	131.95	1.42	0.413
Voltage	2	178.2	89.11	0.96	0.510
Welding Speed	2	2344.7	1172.35	12.63	0.073
Residual Error	2	185.6	92.81		
Total	8	2972.5			

Table 7: ANOVA table of weld width

Source	Degree of Freedom	Sum of Squares	Mean	F-Value	P-Value
Arc Current	2	215.9	107.96	1.44	0.410
Voltage	2	140.2	70.09	0.94	0.517
Welding Speed	2	1906.2	953.11	12.72	0.073
Residual Error	2	149.8	74.92		
Total	8	2412.2			

Table 8: ANOVA table of the depth of penetration

Source	Degree of Freedom	Sum of Squares	Mean	F-Value	P-Value
Arc Current	2	0.9294	0.46468	11.92	0.077
Voltage	2	0.0655	0.03274	0.84	0.543
Welding Speed	2	12.6530	6.32648	162.31	0.073
Residual Error	2	0.0780	0.03898		
Total	8	13.7258			

3.2 S/N ratio

Figure 2 shows the S/N ratio analysis for weld bead dimension obtained from the Taguchi method analysis for weld height, weld width, and depth of penetration. The standard deviation to the mean (signal) ratio was the S/N ratio (noise). The welding speed had the biggest delta value followed by voltage and current. This suggests that the welding speed is the most important factor, followed by arc current and voltage. The S/N ratio is commonly employed assuming that nominal is better, smaller is better, and larger is better. The larger the qualities, the better it is which indicates that high weld height and weld width of single weld layer deposit is preferable, as shown in Table 9 and Table 10. Meanwhile, the penetration depth is selected according to the assumption that the smaller, the better as in Table 11. This research supports the findings of [14-15], who discovered that altering welding parameters resulted in mechanical characteristics in which heat input was reduced by increasing welding current while weld voltage was raised by increasing welding speed.

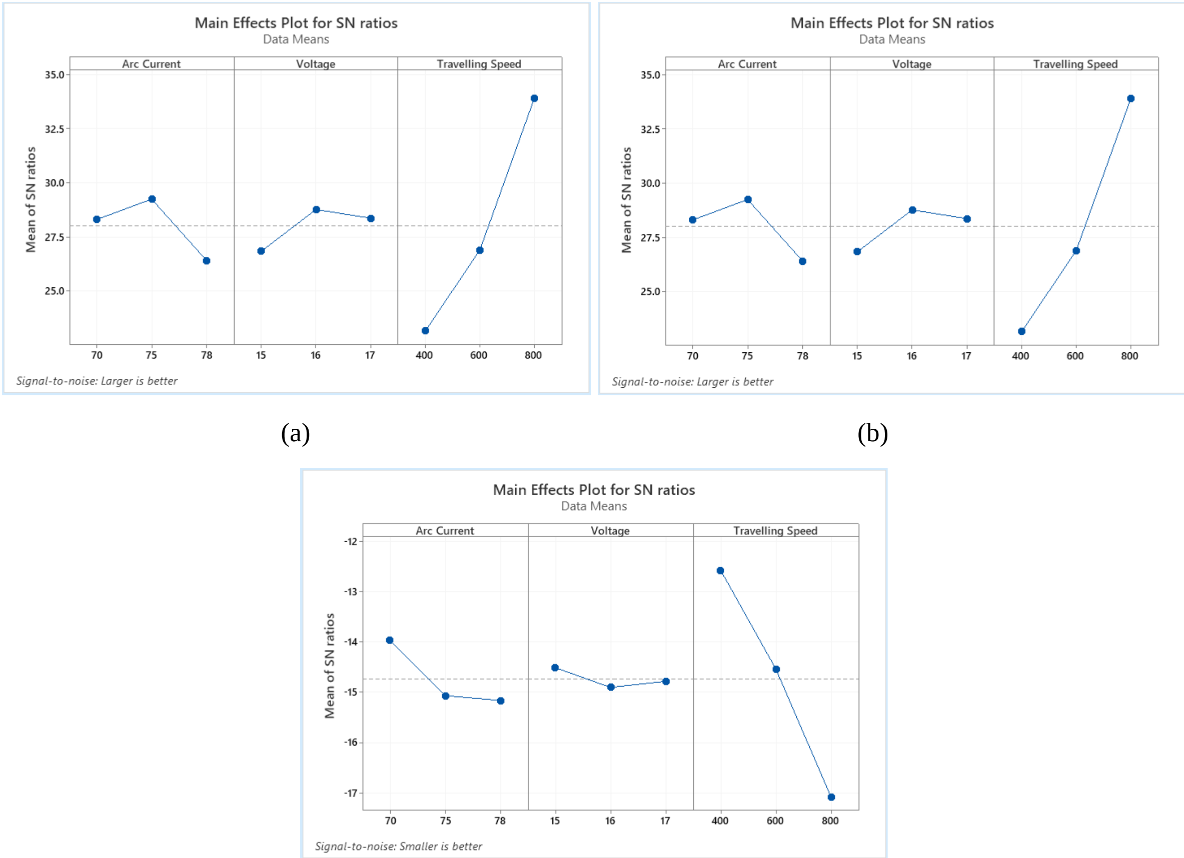

(a) (b)

(c)

Figure 2. Main Plot Graphs of (a) Weld Height; (b) Weld Width; and (c) Depth of Penetration

As can be observed, welding speed (mm/min) had the most significant impact on the experimental analysis of S/N ratio, followed by arc current (A), and finally voltage (V). This was due to the fact that greater welding speed resulted in a decrease of heat input. The rise in mechanical properties demonstrated this. The parameters selected were observed where the voltage and weld current were the major effects on bead width [16], while weld current and welding speed significantly affected bead height in Smart Weld Simulation.

In this research upon 304L stainless steel material base plate on 308L stainless steel filler wire, the effect of the weld layer deposits was investigated on the depth of penetration upon microstructure on a single deposits weld layer [17-18]. The grain orientation and heat input had a significant impact on the WAAM process' mechanical characteristics. Some studies relate heat input to mechanical characteristics. The research primarily focused on the hardness and tensile strength of WAAM-manufactured structures [19]. Commonly, the mechanical properties of the weld deposits are investigated through the microhardness. Since the coldArc GMAWAM involved the least heat input, it was necessary to determine whether or not the cooling approach resulted in better weld bead depositions. The microstructure of the WAAM process changed dramatically as a result of the different heat input and cooling rates.

Table 9: S/N ratio of weld height

Level	**Arc Current (A)**	**Voltage (V)**	**Welding Speed (mm/min)**
1	28.31	26.85	23.18
2	29.25	28.77	26.91
3	26.43	28.37	33.91
Delta	2.82	1.93	10.73
Rank	2	3	1

Table 10: S/N ratio of weld width

Level	Arc Current (A)	Voltage (V)	Welding Speed (mm/min)
1	28.12	26.59	23.10
2	28.83	28.40	26.69
3	26.13	28.10	33.29
Delta	2.70	1.80	10.20
Rank	2	3	1

Table 11: S/N ratio of depth of penetration

Level	Arc Current (A)	Voltage (V)	Welding Speed (mm/min)
1	-13.97	-13.17	-13.03
2	-15.06	-13.18	-15.18
3	-15.16	-13.13	-11.28
Delta	1.19	0.39	4.49
Rank	2	3	1

3.3 Contour plot relationship

The contour plot depicts two-dimensional contours, a three-dimensional surface graphic approach based on constant z variables. The contour plots shown in Figure 3 are topographical maps created from three-dimensional data. The horizontal axis represents welding speed, whereas the vertical axis represents welding voltage. A colour gradient and isolines depict the welding current. In dark green, it also indicates the most significant value of the variables, which appears on each side of the figure. These graphs demonstrate the minimums and maximum in a collection of three-parameter three data. The graph shows each response factor at each level. It is self-evident that when the voltage rises, the current increases as well. On the other hand, increasing welding speed at the same time increases the voltage. The irradiation period decreases as the weld speed increases, resulting in minimal heat input to the weld zone and lower weld penetration depth.

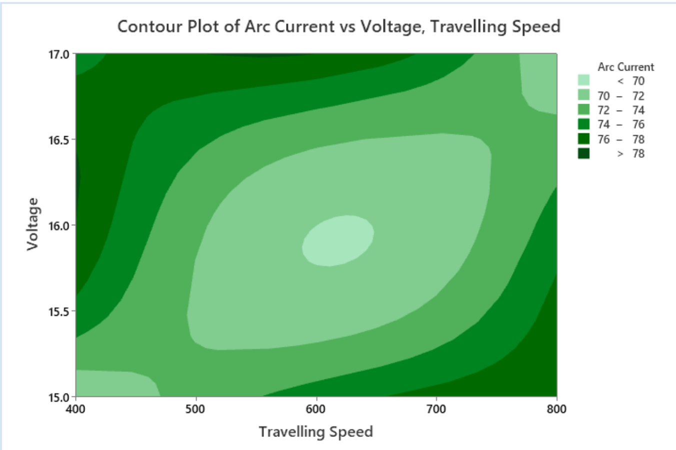

Figure 3. Current versus Voltage Iteration and Welding Speed of Depth of Penetration

Table 13: Smart Weld Software Simulation on Effect of Parameters

Variables	Weld Height (mm)	Weld Width (mm)	Depth of Penetration (mm)
Arc Current	Medium	Medium	Medium
Voltage	Medium	Medium	Low
Welding Speed	High	High	Medium

The data attributed can be supported by a few past studies. A few previous studies backed up the claims made. According to [20], the correct current choice provides a better deposition rate and penetration on the weld material. The high deposition rate and good penetration enhance the material's strength. Also, according to [21] and [22], as the voltage rises, the material's mechanical strength and hardness rise as well. Overall result on simulation Smart Weld output response data is shown in Table 13. This research demonstrated the good penetration of weld bead, where an average 75 A, 16 V, and 800 mm/min setting yielded a sound output of sample strength. Thereby, the expected range of sample strength was 500MPa with the largest value of 56.2 mm, 58.3 mm, and 30.1 mm for bead width, 59.2 mm, 64.6 mm, and 31.9 mm for bead height while the smallest value for depth of penetration is 3.8 mm, 4.35 mm, and 4.67 mm for the first level, second level, third level simulation, respectively. In addition, a welding speed influences the rate of heat input and welding penetration [23-24] and [25]. Overall, the above response table shows that welding speed is the most crucial factor in the welding process, which is influenced by the percentage factor contribution obtained from the ANOVA study [26].

4.0 CONCLUSION

Current, voltage, and welding speed are the input to perform AM, while the depth of penetration and weld bead dimension (height and width) are the output of the Smart Weld Software simulation. The best parameters of stainless steel on coldArc GMAW and the analysis using the Taguchi approach are highly effective in tabulating the collection of parameters into a well-organized design matrix and controlling the number of experimental runs. The main conclusion of the study is summarized as follows:

- The most significant impact of weld height was altered at medium current, medium voltage, high welding speed, and high temperature for the weld bead dimension. At the same time, maximum width varied depending on welding current, voltage, and speed. At medium current, low voltage, and medium welding speed, the effect of parameter affected the depth of penetration.
- The parameter that contributes the most to the coldArc GMAW process with the contribution of AM technology is low input power which is recommended for the optimum temperature advice with low heat involved.
- From the main mean major effect plot of S/N ratios, the best parameters for WAAM were welding speed, followed by arc current and voltage, in which the weld bead dimension tends to change in response to the rate of temperature. Therefore, the deposition rate increases as the heat input increases, resulting in a bigger bead and deeper penetration.
- The dimension was more significant than the actual plate thickness according to the weld height, maximum width, and maximum depth data. This is because the Smart Weld software has almost 70% offsets, and it is recommended to run a validity test to prove the data are significant with the result. However, the welding parameters must be modified based on the material and its impact on the material's mechanical properties.

ACKNOWLEDGEMENT

The authors would like to thank the Faculty of Manufacturing Engineering, Universiti Teknikal Malaysia Melaka (UTeM), for educational and technical support throughout this research. This research is funded through a grant numbered KHAS-KKP/2021/FKP/C00006.

REFERENCES

[1] V. T. Le, D. S. Mai, T. K. Doan and H. Paris, "Wire and arc additive manufacturing of 308L stainless steel components: Optimization of processing parameters and material properties," *Eng. Sci. Technol. an Int. J.*, vol. 24, no. 4, pp. 1–12, 2021, doi: 10.1016/j.jestch.2021.01.009.

[2] J. Müller *et al.*, "Design and parameter identification of wire and arc additively manufactured (WAAM) steel bars for use in construction," *Metals (Basel).*, vol. 9, no. 7, 2019, doi: 10.3390/met9070725.

[3] E. Karayel and Y. Bozkurt, "Additive manufacturing method and different welding applications," *J. Mater. Res. Technol.*, vol. 9, no. 5, pp. 11424–11438, 2020, doi: 10.1016/j.jmrt.2020.08.039.

[4] L. Ji, J. Lu, C. Liu, C. Jing, H. Fan, and S. Ma, "Microstructure and mechanical properties of 304L steel fabricated by arc additive manufacturing," *MATEC Web Conf.*, vol. 128, 2017, doi: 10.1051/matecconf/201712803006.

[5] T. A. Rodrigues, V. Duarte, R. M. Miranda, T. G. Santos, and J. P. Oliveira, "Current status and perspectives on wire and arc additive manufacturing (WAAM)," *Materials (Basel).*, vol. 12, no. 7, 2019, doi: 10.3390/ma12071121.

[6] J. Wanwan, Z. Chaoqun, J. Shuoya, T. Yingtao, W. Daniel, and L. Wen, "Wire Arc Additive Manufacturing of Stainless Steels: A Review," *Appl. Sci.*, 2020.

[7] J. Stuzer, T. Totzauer, B. Wittig, M. Zinke, and S. Juttner, "GMAW Cold Wire Technology for Adjusting the Manufactured Duplex Stainless Steel Components," *Metals (Basel).*, vol. 9, no. 5, pp. 564–583, 2019.

[8] Ivántabernero, A. Paskual, P. Álvarez, and A. Suárez, "Study on Arc Welding Processes for High Deposition Rate Additive Manufacturing," *Procedia CIRP*, vol. 68, no. April, pp. 358–362, 2018, doi: 10.1016/j.procir.2017.12.095.

[9] J. W. Elmer and G. Gibbs, "The effect of atmosphere on the composition of wire arc additive manufactured metal components," *Sci. Technol. Weld. Join.*, vol. 24, no. 5, pp. 367–374, 2019, doi:

10.1080/13621718.2019.1605473.

[10] S. D. Sabdin, N. I. S. Hussein, M. K. Sued, M. N. Ayof, M. S. Ayob, and M. A. S. Abdul Rahim, "Weld bead reinforcement on cold rolled carbon steel sheet joint using ColdArc technology," *Proceedings of the Mechanical Engineering Research Day 2018*, 2018, pp. 197–198, 2018.

[11] N. Ghosh, P. K. Pal, and G. Nandi, "GMAW dissimilar welding of AISI 409 ferritic stainless steel to AISI 316L austenitic stainless steel by using AISI 308 filler wire," *Eng. Sci. Technol. an Int. J.*, vol. 20, no. 4, pp. 1334–1341, 2017, doi: 10.1016/j.jestch.2017.08.002.

[12] S. D. Sabdin, N. I. S. Hussein, M. K. Sued, M. S. Ayob, M. A. S. A. Rahim, and M. Fadzil, "Effects of ColdArc welding parameters on the tensile strengths of high strength steel plate investigated using the Taguchi approach," *J. Mech. Eng. Sci.*, vol. 13, no. 2, pp. 4846–4856, 2019, doi: 10.15282/jmes.13.2.2019.06.0403.

[13] F. Michel, H. Lockett, J. Ding, F. Martina, G. Marinelli, and S. Williams, "A modular path planning solution for Wire + Arc Additive Manufacturing," *Robot. Comput. Integr. Manuf.*, vol. 60, no. April, pp. 1–11, 2019, doi: 10.1016/j.rcim.2019.05.009.

[14] S. Ríos, P. A. Colegrove, F. Martina, and S. W. Williams, "Analytical process model for wire + arc additive manufacturing," *Addit. Manuf.*, vol. 21, no. August 2017, pp. 651–657, 2018, doi: 10.1016/j.addma.2018.04.003.

[15] N. V Amudarasan, K. Palanikumar, and K. Shanmugam, "Impact behaviour and Micro Structural Analysis of AISI 316L Stainless Steel Weldments," *Int. J. Appl. or Innov. Eng. Manag.*, vol. 2, no. 6, pp. 269–272, 2013.

[16] S. Manokruang, F. Vignat, M. Museau, and M. Linousin, "Model of weld beads geometry produced on surface temperatures by Wire and Arc Additive Manufacturing (WAAM)," *IOP Conf. Ser. Mater. Sci. Eng.*, vol. 1063, no. 1, p. 012008, 2021, doi: 10.1088/1757-899x/1063/1/012008.

[17] N. A. Rosli, M. R. Alkahari, M. F. bin Abdollah, S. Maidin, F. R. Ramli, and S. G. Herawan, "Review on effect of heat input for wire arc additive manufacturing process," *J. Mater. Res. Technol.*, vol. 11, pp. 2127–2145, 2021, doi: 10.1016/j.jmrt.2021.02.002.

[18] N. A. Rosli, M. R. Alkahari, F. R. Ramli, M. N. Sudin, and S. Maidin, "Influence of Process Parameters in Wire and Arc Additive Manufacturing (WAAM) Process," *J. Mech. Eng.*, vol. 17, no. 2, pp. 69–78, 2020.

[19] J. L. Prado-Cerqueira *et al.*, "Analysis of favorable process conditions for the manufacturing of thin-wall pieces of mild steel obtained by wire and arc additive manufacturing (WAAM)," *Materials (Basel).*, vol. 11, no. 8, 2018, doi: 10.3390/ma11081449.

[20] P. Long, D. Wen, J. Min, Z. Zheng, J. Li, and Y. Liu, "Microstructure evolution and mechanical properties of a wire-arc additive manufactured austenitic stainless steel: Effect of processing parameter," *Materials (Basel).*, vol. 14, no. 7, 2021, doi: 10.3390/ma14071681.

[21] M. Liberini *et al.*, "Selection of Optimal Process Parameters for Wire Arc Additive Manufacturing," *Procedia CIRP*, vol. 62, pp. 470–474, 2017, doi: 10.1016/j.procir.2016.06.124.

[22] A. Waqas, X. Qin, J. Xiong, H. Wang, and C. Zheng, "Optimization of process parameters to improve the effective area of deposition in GMAW-based additive manufacturing and its mechanical and microstructural analysis," *Metals (Basel).*, vol. 9, no. 7, 2019, doi: 10.3390/met9070775.

[23] F. Montevecchi, G. Venturini, A. Scippa, and G. Campatelli, "Finite Element Modelling of Wire-arc-additive-manufacturing Process," *Procedia CIRP*, vol. 55, pp. 109–114, 2016, doi: 10.1016/j.procir.2016.08.024.

[24] L. M. Wahsh *et al.*, "Parameter selection for wire arc additive manufacturing (WAAM) process," *Mater. Sci. Technol. 2018, MS T 2018*, no. January 2019, pp. 78–85, 2018, doi: 10.7449/2018/MST_2018_78_85.

[25] R. A. Ribeiro, P. D. C. Assunção, E. B. F. Dos Santos, A. A. C. Filho, E. M. Braga, and A. P. Gerlich, "Application of cold wire gas metal arc welding for narrow gap welding (NGW) of high strength low alloy steel," *Materials (Basel).*, vol. 12, no. 3, 2019, doi: 10.3390/ma12030335.

[26] V. K. Modi and D. A. Desai, "Review of Taguchi Method, Design of Experiment (Doe) & Analysis of Variance (Anova) for Quality Improvements Through Optimization in Foundry," vol. 5, no. 1, pp. 184–194, 2018.